

From Optimization to Prediction: Transformer-Based Path-Flow Estimation to the Traffic Assignment Problem

Mostafa Ameli^{a,b}, Van Anh Le^a, Sulthana Shams^a, Alexander Skabardonis^b

^aUniv. Gustave Eiffel, COSYS, GRETTIA, Paris, France

^bInstitute of Transportation Studies, University of California, Berkeley, USA

Abstract

The traffic assignment problem is essential for traffic flow analysis, traditionally solved using mathematical programs under the Equilibrium principle. These methods become computationally prohibitive for large-scale networks due to non-linear growth in complexity with the number of OD pairs. This study introduces a novel data-driven approach using deep neural networks, specifically leveraging the Transformer architecture, to predict equilibrium path flows directly. By focusing on path-level traffic distribution, the proposed model captures intricate correlations between OD pairs, offering a more detailed and flexible analysis compared to traditional link-level approaches. The Transformer-based model drastically reduces computation time, while adapting to changes in demand and network structure without the need for recalculation. Numerical experiments are conducted on the Manhattan-like synthetic network, the Sioux Falls network, and the Eastern-Massachusetts network. The results demonstrate that the proposed model is orders of magnitude faster than conventional optimization. It efficiently estimates path-level traffic flows in multi-class networks, reducing computational costs and improving prediction accuracy by capturing detailed trip and flow information. The model also adapts flexibly to varying demand and network conditions, supporting traffic management and enabling rapid ‘what-if’ analyses for enhanced transportation planning and policy-making.

Keywords: Traffic Assignment, Transformer, Network equilibrium, Traffic flow prediction, Path-based analysis

1. Introduction

The *Traffic Assignment Problem (TAP)* is a process of determining the propagation of flows over the transportation network. The goal is to calculate the network state, given the travel demand between various *origin-destination (OD)* pairs and the network’s capacity constraints (Yosef Sheffi, Prentice-Hall, 1986). Traditionally, this problem is solved through mathematical programs under the *User Equilibrium (UE)* principle, which assumes drivers possess perfect information and make fully rational choices (Wardrop, 1952). Despite potential deviations from reality, this approach consistently provides reasonable solutions to the traffic assignment problem (Bar-Gera, 2002; Jafari et al., 2017). However, the computation for determining optimal solutions in large traffic networks is prohibitively costly. This is because the problem’s complexity grows non-linearly with the increase in the number of OD pairs and directly depends on feasible paths. When the size of the network (the number of links and nodes in a representative graph) increases, allowing us to explore more paths, the number of feasible paths also increases, and the OD demand matrix may grow accordingly, leading to a non-linear increase in computation time (Patriksson, 2015). Because changing the input (demand and graph) results in a new problem to be solved, it requires re-calculation. Therefore, there is a critical need to find another way to capture the complex nature of traffic flow and demand in large networks in order to use the already-solved problem to estimate the solution to the new problem.

Mathematically, the UE, is typically calculated using optimization methods such as the gradient method or fixed-point algorithm (Tan et al., 2020; Mehrabipour and Hajbabaie, 2021; Liu et al., 2023), e.g., Frank-Wolfe algorithm Fukushima (1984). However, with the presence of data-driven approaches and the application of machine learning, an alternative solution to this problem could be prediction instead of optimization. In other words, we can employ supervised learning to learn the optimal solution and predict it given a new demand or a new graph. Recently, a few studies have tried to estimate the link flow solution of UE using machine learning (W. et al., 2023; Rahman and Hasan, 2023; Liu and Meidani, 2024; Liu et al., 2025; Liu and Meidani, 2025; Hu and Xie, 2025) with graph neural networks

(GNNs) emerging as a particularly popular approach for utilising network topology to capture spatial dependencies. For example, [Rahman and Hasan \(2023\)](#); [Liu et al. \(2025\)](#) uses graph convolutional neural networks (GCN) to forecast traffic flow patterns, while [Liu and Meidani \(2024\)](#); [Hu and Xie \(2025\)](#) employed graph attention networks (GATs) to accelerate assignment across large-scale planning scenarios. While promising, GNNs are constrained by their reliance on local message passing, which limits their ability to model long-range dependencies. Deeper stacking can address this, but at the cost of higher computation and over-smoothing of features.

Other approaches have pursued surrogate formulations of the traffic assignment problem. For instance, [Zhang and Qian \(2025\)](#) introduced a low-rank approximation for path-based network models, generating hypothetical path sets based on flows rather than topological structure. [Liu et al. \(2023\)](#) proposes an end-to-end learning framework that embeds the traffic equilibrium problem as a Variational Inequality (VI) layer, producing flows through an iterative equilibrium procedure. Yet these methods remain tied to surrogate calibration or traditional iterative equilibrium procedures.

To address these limitations, we introduce a Transformer-based framework for TAP that employs global self-attention, enabling each element of the input sequence to dynamically weigh its relevance to all others and capture complex, long-range dependencies across the network. The attention mechanism allows the model to selectively prioritize OD pairs with nonzero demand or links with critical features while maintaining global context, enhancing learning efficiency. In contrast, prior TAP models using GAT-based encoder-decoder architectures restrict attention to local neighborhoods and decode flows through MLP layers, limiting their ability to model global interactions ([Hu and Xie, 2025](#)).

Most existing approaches emphasize link-level predictions, leaving path-level demand propagation underexplored despite its importance for understanding traveler behavior. The proposed model predicts detailed path-level flows, enabling an understanding of demand propagation and facilitating flexible ‘what-if’ analyses, i.e., scenario-based evaluations of the effects of simulated changes in network topology or OD demand. By predicting flows at the path level, the model captures the interactions between different OD pairs, overcoming the limitations of link-based approaches that fail to account for these interdependencies. The model learns this mapping in a fully data-driven manner by observing feasible path flows that inherently respect flow conservation and link capacity constraints, producing physically and operationally feasible network states.

Existing neural network approaches are mostly trained and evaluated on familiar scenarios and in single-class networks, leaving their performance under new or unforeseen traffic or network conditions largely unexplored. While Deep Neural Networks (DNNs) have proven effective in domains such as computer vision and NLP [Wang et al. \(2022\)](#), and are increasingly applied to transportation forecasting, the use of sequence-based architectures, particularly Transformers, remains largely unexplored in TAP ([Wen et al., 2023](#); [Xue et al., 2025](#); [Jia et al., 2025](#)). This study addresses these gaps by estimating equilibrium flows in multi-class networks and across diverse demand patterns and network-change scenarios, offering both efficiency and robustness in complex traffic scenarios. To the best of our knowledge, this is the first TAP framework to employ a Transformer-based sequence learning approach incorporating both encoder and decoder global attention.

To summarize, the major contributions of this work are as follows: (i) A Transformer-based model is proposed for directly learning and predicting UE path flow distributions in both single- and multi-class traffic networks; (ii) The model incorporates both network topology and detailed OD demand information, allowing it to generalize to unseen demand patterns and network changes; (iii) Our approach eliminates the computationally intensive optimization step, providing solutions orders of magnitude faster than traditional methods; and (iv) The model supports robust ‘what-if’ scenario analysis under extreme perturbations, where link-removal based topology changes, missing-link observation cases, as well as multi-class and large-scale network applications particularly in terms of OD demand are considered jointly with incomplete OD demand.

The paper is structured as follows: [Section 2](#) presents a summary of relevant literature in the field of traffic assignment and deep learning to better position this paper. [Section 3](#) compares the proposed transformer-based model with other state-of-the-art TAP models. [Section 4](#) formalizes the problem and describe detail model architecture. Numerical experiments are conducted on the Manhattan-like network, Sioux Falls, and Eastern-Massachusetts network in [Section 5](#). Finally, [Section 6](#) concludes the paper.

2. Related literature

The problem of traffic flow prediction and traffic assignment has been extensively studied, with solutions that could be categorized into analytical and data-driven approaches. Analytical methods rely on mathematical formulations and traffic theories to model and solve traffic problems.

Beginning with Wardrop's UE principle and the convex optimisation formulation of Beckmann et al, these approaches laid the foundation of the TAP (Wardrop, 1952; Beckman and McGuire, 1956). To reduce the need for full path enumeration, some analytical approaches developed link-based algorithms, which directly solve for link flows (Fukushima, 1984), as well as column and bush-based methods, which aim to find only promising subsets of paths to improve efficiency (Ford and Fulkerson, 1958; Bar-Gera, 2002; Dial, 2006). Despite these advances, TAP remains computationally intensive for large networks, where evaluating thousands of ‘what-if’ scenarios can take days. This motivates the shift toward supervised machine learning models trained on solver-generated solutions, offering significantly faster inference while retaining the accuracy of the underlying optimization framework.

These approaches integrate machine learning with optimization, where a solver guides training or inference. Models are trained on solver-generated optimal flows to predict link or path flows efficiently (Su et al., 2021; Liu et al., 2023; Rahman and Hasan, 2023). These data-driven approaches employed the power of machine learning to extract patterns from vast amounts of traffic data (Wen et al., 2023; Kipf and Welling, 2017). To predict the optimal solution, machine learning approaches learn path flow distribution under UE conditions. Various machine learning models have been developed for traffic flow prediction, including Graph Neural Networks (GNNs), Heterogeneous Graph Neural Networks (HGNNs), and other deep learning frameworks like Transformer and Recurrent Neural Network (RNN). GNNs and HGNNs excel at representing spatial dependencies and interactions within the network structure (Skardal et al., 2021), while Transformers offer flexibility and efficiency in handling large-scale data with complex spatial-temporal relationships (Wen et al., 2023). As we explore these approaches, it becomes evident that each model offers unique advantages and limitations, making the choice of model highly dependent on the specific characteristics of the traffic prediction tasks. The following sections review studies related to GNN-based methods and Transformer models as deep learning approaches. We examine their advantages and drawbacks to determine which method is more reliable for our approach.

2.1. Graph Neural Networks (GNNs)

GNN is a powerful framework for learning representations of graphs (Kipf and Welling, 2017). They operate through a neighborhood aggregation scheme, where each node’s representation is computed by sampling and aggregating features from its neighboring nodes. This process allows GNNs to capture the structural and relational information inherent in graph data (Kipf and Welling, 2017; Hamilton et al., 2017). Nishi et al. (2018) developed a traffic signal control algorithm based on graph convolutional networks (GCN) and reinforcement learning. Yu et al. (2018) introduced a spatio-temporal GCN to predict urban traffic flows, capturing both spatial and temporal correlations. However, the grid-based convolutional neural network (CNN) models cannot fully capture the intricate structures of transportation systems. Besides, these models inadequately account for variations in the transportation network, such as reductions in link capacity due to traffic accidents or lane closures for maintenance.

Recently Liu and Meidani (2024, 2025) proposed a framework utilizing HGNN for end-to-end traffic assignment and traffic flow learning. They integrated spatial information into the graph representation of transportation networks, enabling feature extraction and aggregation for traffic flow predictions. Fang et al. (2021) developed a traffic flow prediction model using graph attention networks to capture spatial dependencies in traffic networks. Guo et al. (2019) used an attention mechanism to capture the dynamics of spatial dependencies and temporal correlations. A recent work, Hu and Xie (2025), introduced an encoder-decoder transformer-inspired GAT framework that leverages attention mechanisms to map network features to link or path flows. However, their framework still relies on surrogate model calibration by equilibrium-based solution algorithms. We propose to directly solve for path flow even in multi-class network. While these models have demonstrated promising performance, they still face scalability challenges due to computational complexity and memory requirements, as capturing long-range dependencies requires stacking multiple layers (Li et al., 2018; Chen et al., 2020; Zhou et al., 2020).

2.2. Deep Learning (DL) models

[Liu et al. \(2023\)](#) introduced an end-to-end learning framework for user equilibrium (UE) using implicit neural networks. Their approach directly learns travel choice preferences from data and captures equilibrium conditions with a neural network-based variational inequality. However, their method does not approach equilibrium on the flow side to determine the network state. Secondly, they still rely on iterative optimization to calculate solutions rather than directly estimating them, resulting in scalability issues.

Besides the calculation of UE by optimization approaches, there are multiple deep learning approaches for traffic estimation, which can be related to estimating the state of the network. RNNs have been widely used to model temporal dependencies in traffic flow data for prediction. Studies like those by [Bruno et al. \(2020\)](#) and [Wu et al. \(2023\)](#) have shown the ability of Long Short Term Memory (LSTM) networks, a type of RNN, to capture long-term and short-term dependencies in traffic patterns. However RNNs are recursive and cannot parallelize all sequences in parallel, and they are weak for variable-length data ([Ma et al., 2015](#); [Bogaerts et al., 2020](#)). [W. et al. \(2023\)](#) had built a CNN-based model to estimate link flow from incomplete OD data. However, this model was applied on a small-sized dataset of 1000 data points and it does not address the estimation tasks of path flow distribution.

Transformer architectures have shown promise by providing insights into model decisions through attention mechanisms, enabling stakeholders to understand factors influencing traffic patterns ([Mandalis et al., 2025](#)). They have been increasingly applied to traffic flow forecasting tasks ([Wen et al., 2023](#); [Xue et al., 2025](#); [Jia et al., 2025](#)). For instance, [Wen et al. \(2023\)](#) proposed a hybrid model that integrates convolutional neural networks (CNNs) with a Transformer framework to capture both local spatial features and long-range dependencies in traffic flow prediction. However, this approach has some limitations: The proposed architecture is complex, making it infeasible for larger scales because the computation time increases non-linearly. Additionally, the model may struggle to generalize well to different supplies and demands not seen during training, potentially limiting its applicability in real-world traffic management.

Thus, while Transformer models have been widely applied in the context of short-term traffic forecasting, their application to solving TAP remains largely unexplored. This study contributes to this gap by investigating the use of Transformer-based architectures to directly learn path flow distributions under UE conditions.

3. Comparison Between the Proposed Model and Other Neural Network Models

Table 1: Comparison of ML-based approaches in the literature. **Column Descriptions:** **Baseline OD Data** indicates the availability of OD demand; in our work, all perturbations are applied on top of a 30% missing OD training data, reflecting realistic partial demand information. **Perturbations** include: **Multi-class** (predicting flows for multiple vehicle classes); **Link Removal** (simulating abrupt events such as road closures; links removed during testing are not part of training, testing model adaptability; in some studies, partial capacity variations are used instead of full removal); **Link Missing** (links absent from network observations, simulating incomplete network knowledge); and **OD Missing** (partial OD demand observed). **Conservation Handling** is split into two columns: **Link Flow** indicates link-level or node-level conservation, either implicit via path aggregation or diffusion flow modeling across adjacent nodes or explicitly enforced through a loss term; **OD** indicates OD-demand conservation, whether it is implicit by design, enforced via post-processing, or not considered.

Model Type (Reference)	Model Output		Baseline OD Data	Perturbations				Conservation Handling	
	Link Flow	Path Flow		Multi- class	Link Removal	Link Missing	OD Missing	Link Cons.	OD demand
Implicit-layer NN (Liu et al., 2023)	✓		Fixed given 100 %	–	–	✓	✓	Implicit	–
GCN (Rahman and Hasan, 2023)	✓		Fixed given 100 %	–	Capacity Variation	–	–	Implicit	–
HetGAT (Liu and Meidani, 2024)	✓		Fixed given 100 %	–	Capacity Variation	–	✓	Explicit	–
GAT-L, GAT-P (Hu and Xie, 2025)	✓	✓	Fixed given 100 %	–	–	–	✓	Implicit	Post-process
M-HetGAT (Liu and Meidani, 2025)	✓		Fixed given 100 %	✓	✓	–	✓	Explicit	–
Transformer-based (This study)	✓	✓	Missing (30%)	✓	✓	✓	✓	Implicit	Implicit

As discussed in previous sections, the application of neural networks to TAP remains relatively underexplored. Table 1 compares our approach with other state-of-the-art neural network based traffic assignment models in terms of model outputs, handling of perturbations, and flow conservation strategies.

In TAP, flow conservation is essential for physically realistic and equilibrium-consistent predictions, ensuring that OD demand is met and that traffic entering and leaving each node balances correctly. Path-flow formulations, including the approach proposed in this study, respect link flow conservation through path-to-link aggregation, providing feasible equilibrium-consistent solutions (Liu et al., 2023; Hu and Xie, 2025). In contrast, link-based approaches often require explicit enforcement, such as adding node-based conservation terms to the loss function Liu and Meidani (2025), while GCN-based model by Rahman and Hasan (2023) approximates conservation by modelling flow diffusion across neighbours.

While link or path-level flow conservation ensures locally feasible flows, it does not necessarily guarantee that OD demand is satisfied. To address this, Hu and Xie (2025) applied a post-processing step to adjust path flows and enforce OD demand consistency. In contrast, our path-based Transformer model, trained on ground-truth path flows generated under equilibrium conditions, predicts flows that inherently sum to each OD pair's demand, ensuring OD-level conservation without any additional adjustment. Because OD conservation is implicit and learned, no iterative enforcement or adjustment is needed at inference, making predictions potentially faster.

Our evaluation deliberately incorporates extreme network perturbations, such as link removal and missing link observation data, as they provide a rigorous test of the model's generalization capacity and robustness under realistic and challenging conditions. Our model demonstrates robust performance under varying levels of OD data missing levels and link-removal-based topology changes, even without retraining. Further, the studies examine the robustness of the model by either supply or demand side disruptions in isolation, and do not account for simultaneous demand and supply changes, demonstrating more practical and realistic testing conditions. This study addresses these gaps by performing 'what-if' analyses under scenarios involving joint supply-demand perturbations. Missing OD demand is adopted as a baseline perturbation in this work, as it reflects a common and practically unavoidable source of uncertainty in real-world applications. Building on this baseline, we introduce additional perturbations such as link removal or missing link data. Lastly, all of the aforementioned studies focus on single-class network graphs, with the exception of Liu and Meidani (2025), which extends the model to multi-class traffic scenarios. While their methodological framework differs from ours, their choice of test cases is closely aligned with our work. We further extend the evaluation by jointly considering network perturbations with incomplete OD data, demonstrating enhanced adaptability.

This work introduces a Transformer-based sequence learning framework for TAP that directly estimates path-level equilibrium flows in single and multi-class networks. The model inherently satisfies link and OD-level flow conservation, handles joint supply-demand perturbations, and adapts to changes in network topology and demand patterns. By providing a computationally efficient surrogate for traditional optimization solvers, it supports realistic 'what-if' analyses and demonstrates the practical potential of sequence-based architectures for large-scale traffic assignment.

4. Transformer-based model for optimal path flow prediction

4.1. Problem formulation

As mentioned before, the goal is to estimate the optimal solution of path flow distribution from given OD demands and the graph instead of solving it. In mathematical terms, we consider a network represented as a graph $G = (V, E)$, where V stands for the set of nodes with size N , and E for the set of links. Let R represent the set of OD pairs. For each OD pair, denoted by $r \in R$, where $r = (v_1, v_2)$, $\forall v_1, v_2 \in V$, vehicles of class $z \in Z$ can travel via several finite and nonempty feasible paths of path set \mathbf{P}_r . Let n denote the number of classes in the network. Each set $\mathbf{P}_r \in \mathbf{P}^k$ encompasses k feasible paths for each OD pair r . Furthermore, let \mathbf{X} represents OD demand matrix, $x_r^z \in \mathbf{X}$ represents the demand of OD pair r traveled by class z , and $f_{\mathbf{P}_r}^{r,z} \in \mathbf{F}$ represents paths flow distribution of OD pair r on path set \mathbf{P}_r , with class z . Each set $f_{\mathbf{P}_r}^{r,z}$ encompasses k flow values for every OD pair r .

Following the UE principle, the shortest path is the path that has the minimum cost. In the UE solution, all used paths must be at the minimum possible cost (or equal the shortest path). Mathematically, it is equivalent to the following conditions:

$$f_p^{r,z}(c_p^{r,z} - u_r^z) = 0 \quad \forall p \in \mathbf{P}_r, r \in R, z \in Z \quad (1)$$

$$c_p^{r,z} - u_r^z \geq 0 \quad \forall p \in \mathbf{P}_r, r \in R, z \in Z \quad (2)$$

$$\sum_{p \in \mathbf{P}_r} f_p^{r,z} = x_r^z \quad \forall r \in R, \forall z \in Z \quad (3)$$

$$f_p^{r,z} \geq 0, c_p^{r,z} \geq 0, u_r^z \geq 0 \quad \forall p \in \mathbf{P}_r, r \in R, z \in Z \quad (4)$$

where $c_p^{r,z}$ denotes the cost of path p with class z for OD pair r , which equals the sum of the cost of all links in that path (Equation 5), and u_r^z denotes the minimum path travel cost of OD pair r with class z (Equation 6):

$$c_p^{r,z} = \sum_{e \in E} \Delta_{p,e}^{(r)} c_e^z, \quad \Delta_{p,e}^{(r)} = \mathbf{1}\{e \in p\}. \quad (5)$$

$$u_r^z = \min_{\forall p \in \mathbf{P}_r} c_p^{r,z} \quad \forall r \in R, z \in Z \quad (6)$$

where $\Delta_{p,e}^{(r)} \in \{0, 1\}$ indicates whether link e lies on path p for OD pair r , and c_e^z is the class- z link travel time computed via a BPR function:

$$c_e^z = t_{e,0}^z \left(1 + 0.15 \left(\frac{\sum_{z' \in Z} v_e^{z'}}{C_e} \right)^4 \right), \quad (7)$$

where $t_{e,0}^z$ is the free-flow travel time, C_e is the link capacity and $v_e^{z'} = \sum_{r \in R} \sum_{p \in \mathbf{P}_r} \Delta_{p,e}^{(r)} f_p^{r,z'}$ denotes the class-specific link flow aggregated from path flows.

The ultimate goal is to find \mathbf{F}^* , the optimal path flow distribution for UE condition defined by Wardrop (1952). Each set of path flow distribution $f_p^{r,z*} \in \mathbf{F}^*, \forall r, \forall z$ is the optimal solution for OD pair r on path set p_r with class z . Equation 1 shows that for all classes $z \in Z$, the paths connecting any OD pair r can be categorized into two groups: those that carry flow, where the travel time $c_p^{r,z}$ matches the minimum OD travel time u_r^z , and those that do not carry flow, where the travel time is greater than or equal to the minimum OD travel time. Equation 2 ensures that u_r^z is the minimum path cost. Equation 3 ensures that all the demand is served. Equation 4 ensures the positivity of variables. However, this UE solution is only applicable when all drivers have perfect knowledge of the network state. In reality, it is not the case, so normally there will be a delay in the network. In the literature, this imperfection of knowledge is represented by stochastic terms that lead to other equilibrium terms such as Stochastic User Equilibrium (SUE) or Boundedly Rational UE (BRUE) (Ameli et al., 2020).

The model proposed in this study aims to learn a function $\mathcal{F}(\cdot)$ that maps $N^2 \times n$ instances of OD demand matrix \mathbf{X} and $N^2 \times k$ instances of feasible path set \mathbf{P} in graph G , to $N^2 \times kn$ instances of optimal path flow distribution \mathbf{F}^* , defined as Equation 8:

$$\mathcal{F}(G, \mathbf{X}, \mathbf{P}) = \widehat{\mathbf{F}}_{G,\mathbf{X}}^*, \quad (8)$$

where $\widehat{\mathbf{F}}_{G,\mathbf{X}}^*$ is the predicted path flow distribution of the optimal solution \mathbf{F}^* for graph G with demand \mathbf{X} .

4.2. Model architecture

To achieve our goal, we developed a transformer-based framework that includes both Encoder and Decoder blocks. Figure 1 presents the overview of our framework, which includes four main parts: data preprocessing, Encoder, Decoder, and prediction.

Since the data is graph-based, where the graph and OD matrix are conditional inputs, we aim to estimate the optimal solution when we have variations in the graph and demand profile. An Encoder-Decoder architecture offers a robust framework for capturing complex dependencies (Qasim et al., 2022). The Encoder processes the input sequence (a series of OD pairs) and encodes this information into a context vector. The Decoder then uses this context vector to generate the output sequence (path flow distribution). The Encoder-Decoder model can handle varying lengths of

input and output sequences (Ghaderi et al., 2017), which is particularly useful in transportation networks where the number of nodes and links can vary. This flexibility is advantageous for the ‘what-if’ analysis.

In Transformer architectures, the attention mechanism is utilized in both the Encoder and Decoder blocks to enable the model to selectively focus on the meaningful values, and ignore the less meaningful values (Vaswani et al., 2017). The selective focusing in this problem means the model only focuses on the OD pairs that have a demand higher than zero ($x_r^c > 0$) or where there are features of the link between that pair, thereby enhancing the model’s overall performance. Below, we describe the architecture in detail, highlighting how the data is processed through each stage of the model.

4.2.1. Data Preprocessing

To learn the graph, we need to ensure that all features are on the same scale. Since the raw data is not normalized, we perform a preprocessing step to encode the raw features into a lower-dimensional representation. The input tensor is constructed from four tensors. The first tensor stores graph information (link features), including the length and capacity of each link. The second tensor stores free-flow travel time for each link and each class. The third tensor contains the OD demand matrix for each class. The fourth tensor holds the encoded feasible paths information for each OD pair.

Let m denotes the number of link features. For n number of classes and k feasible paths in the network, the dimension a of the input tensor is calculated as: $a = m + 2n + k$. All the notations in this section are presented in Table 2.

After stacking and normalizing these tensors, the resulting input tensor is denoted as $\tilde{\mathbf{I}}$. As shown in the Figure 1,

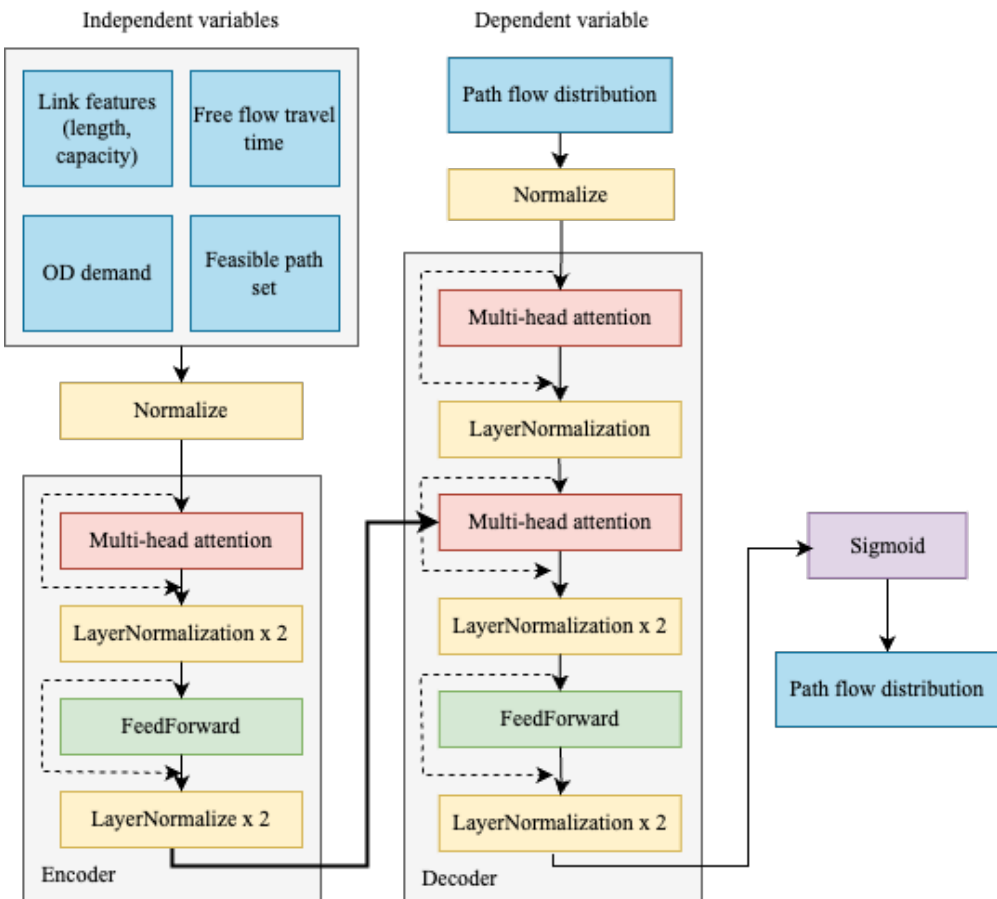


Figure 1: Model architecture

Table 2: List of notations

$G(V, E)$	Transportation network graph
R	OD pairs set
V	Set of nodes in G with size of $ V = N$
E	Set of links in G with size of $ E = L$
Z	Set of classes in G with size of $ Z = n$
m	Number of link features
n	Number of classes in the network
k	Number of feasible paths for each OD pair
a	Input tensor dimension
d	Embedding size
$\mathbf{X} \in \mathbb{R}^{N^2}$	OD demand matrix
$\mathbf{P} \in \mathbb{R}^{N^2}$	Feasible path set
$\tilde{\mathbf{I}} \in \mathbb{R}^{N^2 \times a}$	Normalized input tensor
$\tilde{\mathbf{F}} \in \mathbb{R}^{N^2 \times k}$	Normalized path flow distribution tensor
$\mathbf{F}^* \in \mathbb{R}^{N^2 \times k}$	Optimal path flow distribution tensor
$\hat{\mathbf{F}}^* \in \mathbb{R}^{N^2 \times k}$	Predicted path flow distribution tensor
$\mathbf{W}_Q, \mathbf{W}_K, \mathbf{W}_V$	Learnable weight matrix
\mathbf{B}	Single-head attention output
\mathbf{G}	Multi-head attention output
$\mathbf{W}_o, \mathbf{W}_1, \mathbf{W}_2, \mathbf{W}_3, \mathbf{W}_4$	Parameters of the feed-forward layer
\oplus	Concatenation operator

this normalized tensor $\tilde{\mathbf{I}}$ is then fed into the Encoder block. The path flow distribution \mathbf{F}^* is what our model needs to learn and predict. \mathbf{F}^* is normalized before being fed into the Decoder block. The normalized tensor is $\tilde{\mathbf{F}}$.

4.2.2. Attention Mechanism

As the initial step of feature extraction, we employ a key-query-value mechanism on the input tensor in the Encoder block, and on the output tensor (path flow distribution tensor) in Decoder block, in addition to the weighted sum operation, to capture the importance of each OD pair (see Figure 1). In single-head attention, OD pair features are transformed into key, query, and value matrices, denoted by $\mathbf{K}, \mathbf{Q}, \mathbf{V}$ respectively, via the following linear transformations:

$$\mathbf{Q}, \mathbf{K}, \mathbf{V} = [\tilde{\mathbf{I}}\mathbf{W}_Q, \tilde{\mathbf{I}}\mathbf{W}_K, \tilde{\mathbf{I}}\mathbf{W}_V], \quad \forall \mathbf{W}_Q, \mathbf{W}_K, \mathbf{W}_V \in \mathbb{R}^{a \times d} \quad (9)$$

The value matrix captures the learned representations and importance scores for each pair, the query matrix \mathbf{Q} represents the target pair's characteristics, and the key matrix \mathbf{K} contains the features of other pairs. Attention scores between the query vector and each key are calculated using the scaled dot-product, which is then normalized by a softmax function to ensure the sum of the weights equals to one. These attention scores are subsequently used in a weighted sum operation with the value vector \mathbf{V} (Equation 10), allowing the model to focus on the most relevant output vectors for a given input vector.

$$\text{Attention}(\mathbf{Q}, \mathbf{K}, \mathbf{V}) = \mathbf{B} = \text{softmax}\left(\frac{\mathbf{Q}\mathbf{K}^T}{\sqrt{d\mathbf{K}}}\right)\mathbf{V}, \quad (10)$$

where $d\mathbf{K}$ is the last dimension of the key vector \mathbf{K} , $\mathbf{B} \in \mathbb{R}^{N^2 \times d}$.

For multi-head attention, these steps are repeated h times to produce multiple attention outputs, where h is the number of heads. The attention output tensors are concatenated along the last dimension, and a learnable weight matrix \mathbf{W}_o is applied through Equation 11 to return the final output tensor \mathbf{G} with the same shape as the input tensor

I.

$$\text{Multi-head}(\mathbf{Q}, \mathbf{K}, \mathbf{V}) = \mathbf{G} = \bigoplus_{i=0}^{h-1} \mathbf{B}_i \mathbf{W}_o, \quad \forall \mathbf{W}_o \in \mathbb{R}^{dh \times a} \quad (11)$$

Figure 2 provides a comprehensive illustration of the multi-head attention mechanism's operational details.

4.2.3. Encoder Layers

The Encoder layer consists of two main components: a multi-head attention mechanism and a feed-forward neural network, both followed by residual connections and two layers of normalization. The detailed steps of each encoder layer include adding the output of multi-head attention to the input tensor, called a residual block. This residual connection helps mitigate the vanishing and exploding gradient problems, which are common issues in deep networks. It leads to faster convergence during training because it allows the model to learn identity mappings more easily He et al. (2016). We perform dropout, merge in residual connections, and perform two-layer normalization to stabilize the training process (Equation 12).

$$\mathbf{E}' = \text{LayerNorm}(\text{LayerNorm}(\tilde{\mathbf{I}} + \text{Dropout}(\mathbf{G}))) \quad (12)$$

The output is then passed through a feed-forward neural network with two hidden layers, using ReLU activation functions. The feed-forward layer's output is added to the output of the previous step (the second residual block),

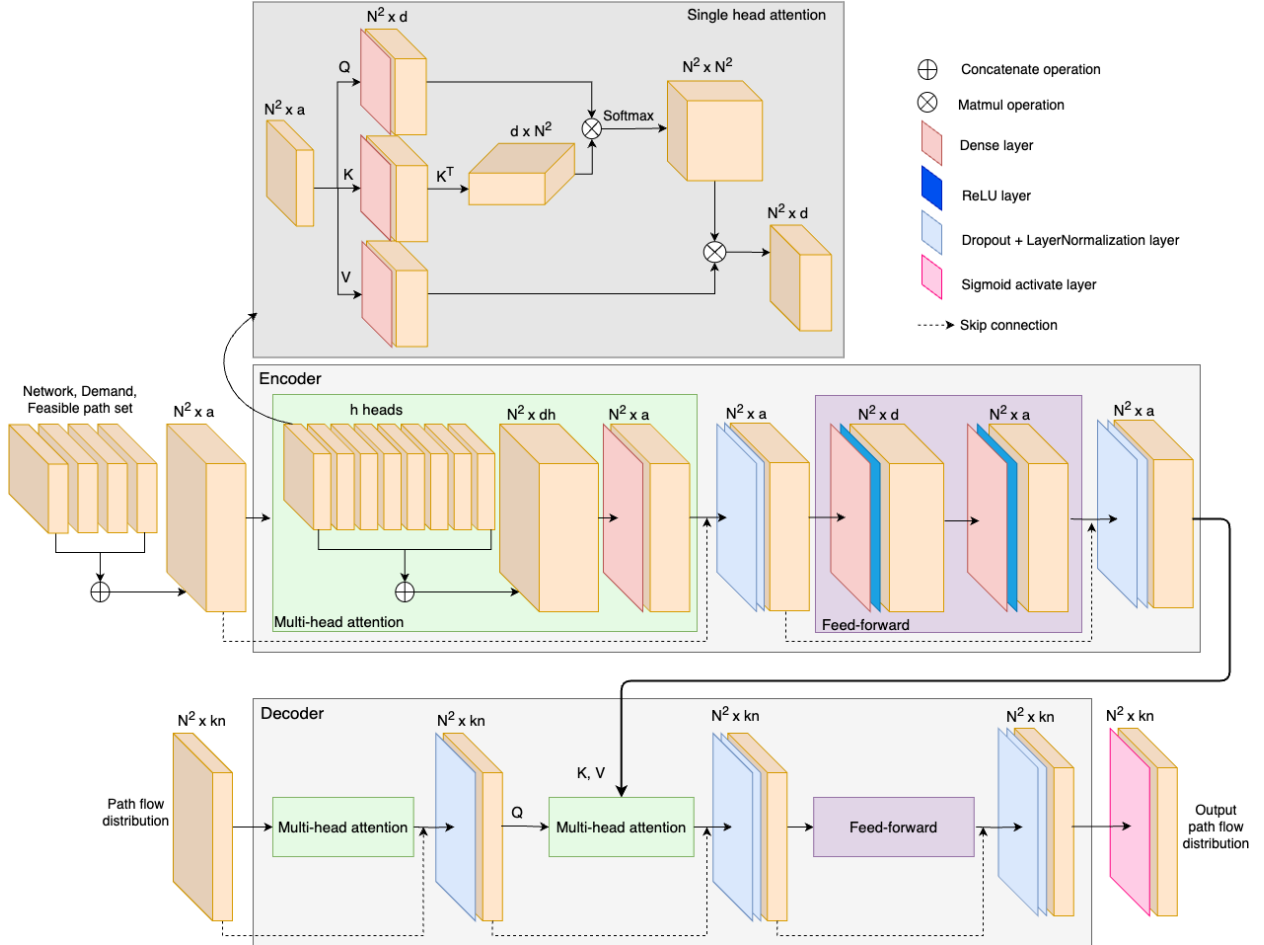


Figure 2: Model detail architecture

followed by another two layers of normalization, [Equation 13](#), to stabilize the training:

$$\mathbf{E} = \text{LayerNorm}(\text{LayerNorm}(\mathbf{E}' + \text{Dropout}(\mathbf{W}_1 \text{ReLU}(\mathbf{W}_2 \mathbf{E}')))), \quad (13)$$

where \mathbf{W}_1 and \mathbf{W}_2 are shared across all the positions in a layer.

Each Encoder layer processes the input tensor sequentially, capturing hierarchical relationships within the network. The encoder block comprises multiple encoder layers stacked together. The output from one encoder layer serves as the input to the next, enabling the model to learn increasingly abstract representations of the input data.

4.2.4. Decoder Layers

The Decoder layer generates the output path flow distribution by attending to both the previous Decoder layer's output and the Encoder's output. Similar to the Encoder, the Decoder starts with multi-head attention on its input. The output of the first multi-head attention block on path flow tensor is denoted by \mathbf{G}_1 . We also apply dropout, residual connection and layer normalization on this output ([Equation 14](#)):

$$\mathbf{D}' = \text{LayerNorm}(\tilde{\mathbf{F}} + \text{Dropout}(\mathbf{G}_1)) \quad (14)$$

The decoder then applies multi-head self-attention using the encoder's output \mathbf{E} as the key and value, and the decoder's multi-head attention output \mathbf{D}' as the query. This allows the decoder to focus on relevant encoder information. \mathbf{G}_2 denotes the output of this second multi-head attention. As shown in [Figure 1](#), the second residual connection and 2 layers of normalization are repeated before going to the feed-forward network ([Equation 15](#)). In [Equation 16](#), the result of the second residual connection is fed to a feed-forward layer, then the third residual connection is applied before the last 2 normalization layers:

$$\mathbf{D}'' = \text{LayerNorm}(\text{LayerNorm}(\mathbf{D}' + \text{Dropout}(\mathbf{G}_2))) \quad (15)$$

$$\mathbf{D} = \text{LayerNorm}(\text{LayerNorm}(\mathbf{D}'' + \text{Dropout}(\mathbf{W}_3 \text{ReLU}(\mathbf{W}_4 \mathbf{D}')))), \quad (16)$$

where \mathbf{W}_3 and \mathbf{W}_4 are shared across all the positions in a layer. The decoder block is composed of multiple decoder layers. The final output of the decoder is a tensor of size $N^2 \times kn$, after a sigmoid activate function, we get a tensor representing the normalized path flow distribution for k feasible paths and c classes of each OD pair:

$$\widehat{\mathbf{F}}^* = \text{sigmoid}(\mathbf{D}) \quad (17)$$

The Encoder and Decoder are two main blocks of this model in order to accomplish the prediction task ([Equation 17](#)). In the next section, we apply the proposed architecture to two test cases with different characteristics. Note that given predicted path flows $\hat{f}_p^{r,z}$, we report:

$$\varepsilon_{\text{OD}} := \frac{1}{|R|n} \sum_{r \in R} \sum_{z \in Z} \left| \sum_{p \in \mathbf{P}_r} \hat{f}_p^{r,z} - x_r^z \right|, \quad (18)$$

$$\varepsilon_{\text{link}} := \frac{1}{|E|} \sum_{e \in E} \left| \sum_{r \in R} \sum_{z \in Z} \sum_{p \ni e} \hat{f}_p^{r,z} - \hat{v}_e^z \right|, \quad (19)$$

$$\phi_{\text{KKT}} := \frac{1}{|R|n} \sum_{r \in R} \sum_{z \in Z} \sum_{p \in \mathbf{P}_r} \hat{f}_p^{r,z} \max(0, c_p^{r,z} - u_r^z), \quad (20)$$

which quantify OD-conservation error, path-to-link aggregation consistency, and complementarity residuals, respectively. The model is penalized during training to ensure that these errors remain negligibly small (ideally near zero).

5. Numerical Experiments

Two numerical experiments are conducted to evaluate the accuracy, efficiency, and generalization capability of the proposed framework. In Section 5.3, We first experiment with a synthetic Manhattan-like network to assess the basic effectiveness of the model. We evaluate the model's performance under conditions of incomplete OD demand. The second experiment in Section 5.4 is on urban transportation networks (Sioux Falls and Eastern-Massachusetts network) with several 'what-if' scenarios to examine robustness against various realistic network perturbation scenarios. The implementation details and datasets used in these experiments are available at https://github.com/VivianeLe/Path_Flow_Prediction. The details of the experiments will be explained in the following sections.

5.1. Training setup

In this study, we compared the performance of various gradient descent optimization algorithms, including Stochastic Gradient Descent (SGD), RMSprop, Adagrad, and Adam. Our findings indicate that the Adam algorithm is the most effective for this research, offering superior accuracy and faster convergence. The model was trained using the Mean Squared Error (MSE) loss function, with the hyperparameters detailed in Table 3. This set of hyperparameters has been validated as particularly effective when employing Transformers on large generated datasets (Chariton et al., 2021).

Table 3: Hyperparameters used for model training

Parameter	Value	Parameter	Value
Batch size	64	Attention heads	8
Dimension	128	Epochs	100
Encoder layers	8	Learning rate	0.001
Decoder layer	1	Dropout rate	0.1

5.2. Model evaluation indicator

To evaluate the performance of the model, four measures are considered, one based on the UE condition and three classical measures. Based on the first condition of UE principle (Equation 1), we calculate the difference of average delay (AD) of the network between the predicted flow and the solution obtained from the optimizer as follows:

$$AD^z = \frac{\sum_{\forall r} \sum_{\forall p} \hat{f}_p^{r,z} (c_p^{r,z} - u_r^z)}{\sum_{\forall r} x_r^z} \quad \forall z \in Z \quad (21)$$

In other words, a smaller difference, ideally close to zero, indicates a better-performing model. Other metrics to evaluate model performance include: mean absolute error (MAE), mean absolute percentage error (MAPE):

$$MAE^z = \frac{1}{y} \sum_{\forall r} \sum_{\forall p} |f_p^{r,z*} - \hat{f}_p^{r,z}| \quad \forall z \in Z \quad (22)$$

$$MAPE^z = \frac{1}{y} \sum_{\forall r} \sum_{\forall p} \left| \frac{f_p^{r,z*} - \hat{f}_p^{r,z}}{f_p^{r,z*}} \right| \times 100\% \quad \forall z \in Z \quad (23)$$

where $f_p^{r,z*}$ and $\hat{f}_p^{r,z}$ respectively represent the "ground truth" (optimal value) and predicted value of path flow, y represents the total number of feasible paths of all OD pairs. It is important to note that while link flows may be unique, path flows are not necessarily so. In particular, when the network is homogeneous, it is not possible to establish a definitive "ground truth" for the distribution of path flows. In such cases, the only means of validating the results is through the use of quality indicators.

5.3. Manhattan-like road network

In this section, we examine the generalization capability of the proposed model to a Manhattan-like network. We consider a realistic scenario where the regional OD demand values are incomplete. In this way, the model is expected to learn the inherent patterns and structures of the transportation network, enabling reliable flow prediction even when parts of the OD demand information are missing, as commonly observed in real-world data collection.

5.3.1. Data description

As part of our experimental setup, we generate a grid network with 25 nodes and 80 links. The detailed information of the link, including capacity, length, and free flow travel time, is randomly generated following uniform distribution (see Table 4). For the 1st analysis, we generate data and train the model with a single class (car). Figure 3 presents the heatmap of link capacity for each link in the bi-directional graph.

Table 4: Manhattan-like road network characteristics

Measure	Min value	Max value
Length (km)	20	40
Capacity (veh)	1000	2000
Free flow time (hour)	0.5	1
Demand	50	500

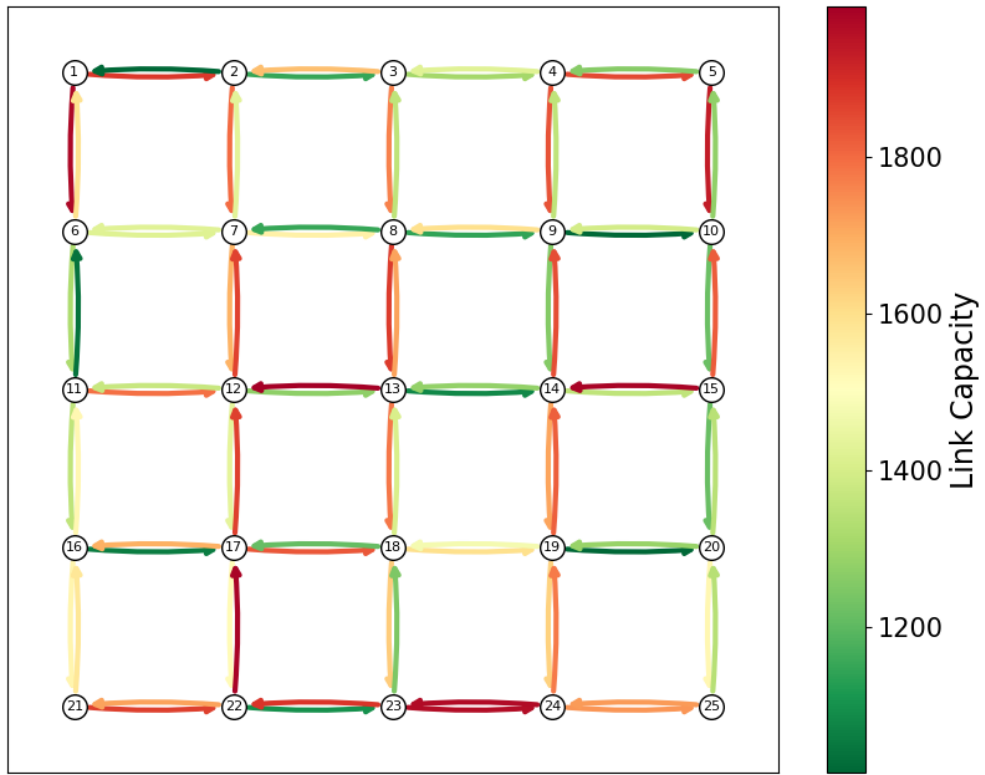


Figure 3: Sampled generalized synthetic networks with 25 nodes and 80 links

For the experiment, incomplete OD demand values are achieved by randomly removing a ratio of OD pairs. Let s denotes the number of complete OD pairs (v_1, v_2) , with $v_1 \neq v_2$, $s = N^2 - N$, j denotes the missing percentage. Two missing ratios are considered in this experiment: $j = 30\%$ and $j = 40\%$. With this experiment, we can perform

‘what-if’ analyses where the demand changes. To create the training, testing, and validation datasets, we generate 4000 OD demand matrices at each missing ratio for the graph ($s - j$ OD pairs). This approach enables the model to learn the inherent patterns and structures of the transportation network, even when some demand information is missing.

In this study, we set $k = 3$ for shortest paths exploration per each OD pair. If an OD pair has fewer than three feasible paths, the path set and path flow are padded with zeros to reach a dimension of three. The optimal solutions for UE of 4000 demand scenarios at each missing ratio are then obtained by utilizing the Gurobi optimizer. The solution has some delays due to the linearization. Because our aim is to learn and estimate the solution accurately, we will accept this error and assume that the network has reached an equilibrium state. The training, validation, and testing sets are then divided into 70%, 20%, and 10%, respectively. We train the model with the missing rate $j = 30\%$, then test the model at two missing rate $j = 30\%$ and $j = 40\%$. Thus, a pre-trained model on $j = 30\%$ was directly applied to predict outcomes under $j = 40\%$ absence, providing a more practical approach for real-world use.

5.3.2. Numerical results

The training history of the model is shown in [Figure 4](#). The model converges smoothly after 80 epochs with few fluctuations. After predicting path flow distribution, the link flows are then aggregated to calculate the error at both path and link levels. [Table 5](#) summarizes the prediction performance of the proposed model under different OD demand missing ratios. When the missing ratio increases, the proposed model maintains a relatively low MAPE. For instance, in the scenario where 30% of OD demand is missing, the MAPEs for predicted link flow and path flow are 2.56% and 5.50%, respectively. When the missing ratio increases to 40%, the model provides link flow and path flow MAPEs of 4.35% and 7.17%, respectively. The average network delay resulting from the predicted path flow remains under 2% in both scenarios, though it does increase as the missing ratio of OD pairs rises. Representing only a slight increase compared to the 30% missing ratio, the model was able to generalize reasonably well to a 10% higher OD missing case without retraining.

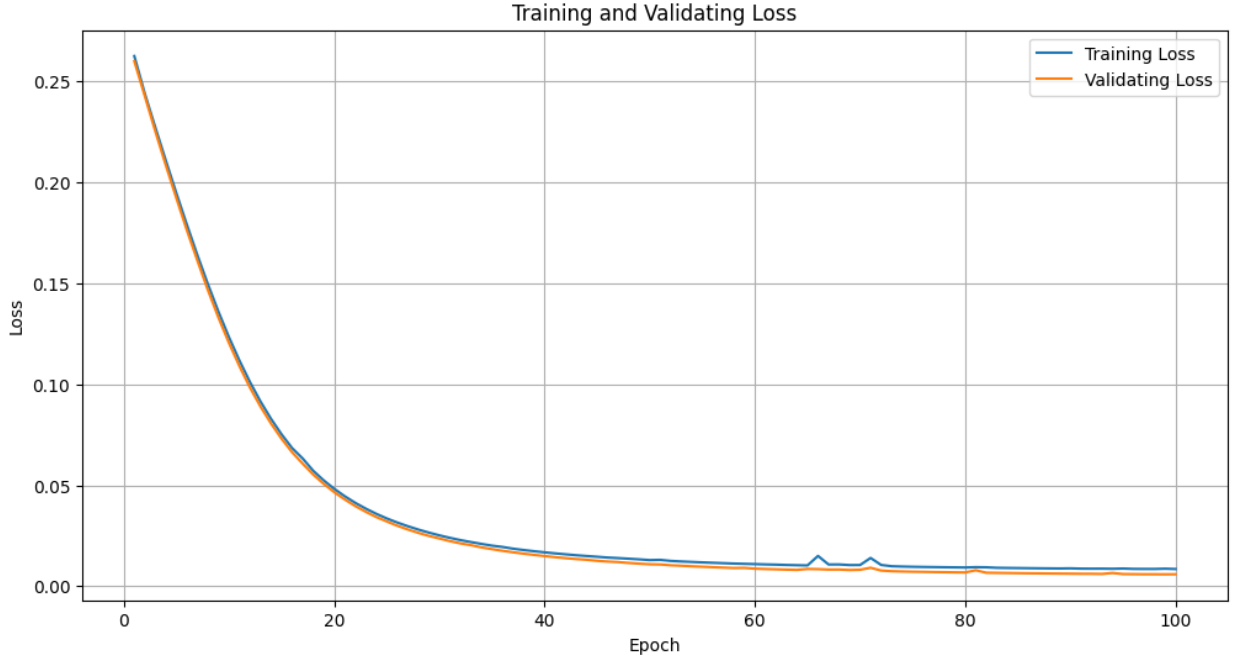


Figure 4: Training history of model with synthetic network

In addition to the prediction accuracy, the training time is also an important factor in evaluating the efficiency and practicality of machine learning models. The training time is 72 minutes, while the time for solving the UE problem with the optimizer is 210 minutes. The prediction time for a single OD demand matrix is 0.001 seconds, it is 5000

Table 5: Model performance under different OD demand missing ratios

Indicator	Missing ratio = 30%	Missing ratio = 40%
Path flow MAE	10.95	18.54
Path flow MAPE (%)	4.50	5.57
Average path cost (mins)	216.62	387.51
Predicted average delay (mins)	2.64	5.34
Delay percentage (%)	1.22	1.38
AD difference (mins)	2.62	4.61

times faster than using the Gurobi optimizer (5 - 7 seconds per OD matrix). These results highlight the computational efficiency of the proposed model in addressing traffic assignment problems.

5.4. Validation on urban transportation network

Having observed the model's strong performance with the synthetic Manhattan-like network, we evaluate its effectiveness on an urban transportation network. This step allows us to assess its effectiveness under more realistic conditions, where traffic systems exhibit greater heterogeneity and complexity. Starting from the baseline scenario of incomplete OD data, we introduce additional training cases that incorporate varying levels of missing information and structural constraints. Corresponding testing sets are then defined for each scenario to systematically examine the model's robustness and adaptability across different urban traffic settings.

Note that the OD demand values and the number of OD demand matrices remain fixed for the analysis. We explore the following scenarios on the urban transportation network:

Scenario 1: Both demand and network supply change

We consider cases with varying link missing ratios alongside partially missing OD demand data. This setup reflects realistic conditions of data unavailability in urban transportation systems, where incomplete or unreliable measurements on both demand and supply sides are common. The scenario is designed to evaluate the model's ability to perform reliably under such simultaneous data limitations.

Scenario 2: Some links in the network are disabled randomly

Specifically, we evaluate the model's performance when 2–3 links are randomly removed from operation. This setup reflects realistic structural disruptions in urban transportation systems, such as road closures due to accidents, construction works, or policy-driven restrictions. Importantly, these cases are tested without retraining the model on the newly disabled links, to assess its ability to generalize to minor unforeseen disruptions in network structure.

Scenario 3: There are multiple classes in the network (car and truck).

This scenario introduces heterogeneity in demand patterns and traffic dynamics, thereby testing the model's ability to account for varying impacts of different vehicle types on network flows.

Scenario 4: When the network scale increases (large-scale network).

Finally, we test the model on a larger-scale urban network to examine its scalability and robustness in more complex settings. Compared to the synthetic and medium-sized urban networks, this scenario involves a greater number of OD pairs, links, and potential sources of congestion. It allows us to assess the model's efficiency and effectiveness when applied to realistic, large-scale transportation systems.

In the following section, we describe the network and experimental setup for each scenario, including the urban network characteristics, OD demand inputs, and the design of training and testing datasets.

Table 6: SiouxFalls network details

Detail	Min value	Max value
Length (km)	2	10
Capacity (vehicle)	4823	25900
Free flow travel time (minutes)	2	10
Demand	100	4000

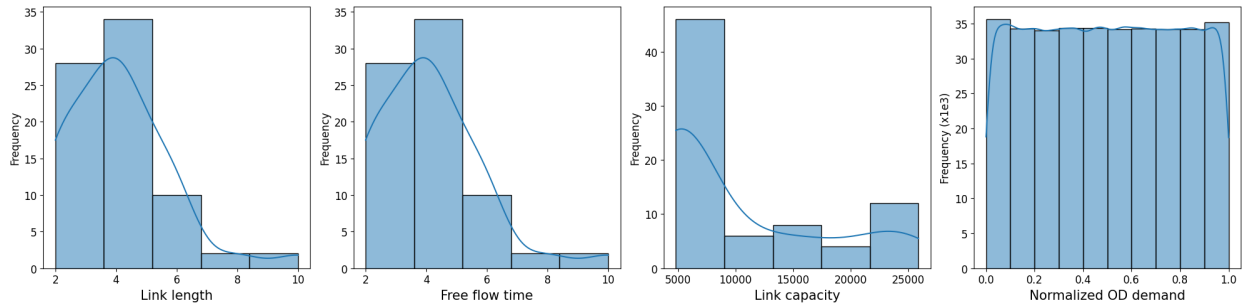


Figure 5: Histogram of Sioux Falls network characteristics with trend line

5.4.1. Data description and Experiment Set-up

In scenarios 1, 2, and 3, we utilize Sioux Falls network. The information about this network is sourced from [H. et al. \(2023\)](#). This network comprises 24 nodes and 76 links. [Table 6](#) and [Figure 5](#) illustrates the network's characteristics.

The original dataset comprises link lengths ranging from 2 to 10 kilometers and free-flow travel times spanning 2 to 10 minutes. The histograms of these two variables exhibit a right-skewed distribution, indicating that the majority of links are shorter in length and have shorter free-flow travel times. Most links have capacities between 5,000 and 10,000, while links with capacities exceeding 20,000 constitute a small percentage of the dataset [H. et al. \(2023\)](#).

In the first scenario of this experiment, to conduct a comprehensive 'what-if' analysis, we combine both the change in demand (incomplete demand) and in network supply (where some links are missing). We use a single-class network in this scenario for simplicity. Let L denotes the number of links, and j denotes the percentage of missing links. We consider that the regional OD demand is missed by 30%, and two link missing ratios are examined: $j = 5\%$ and $j = 10\%$. 4000 different OD demand matrices at this demand missing ratio are generated. The demands follow uniform distribution ([Figure 5](#)). The optimal path flow is then obtained by the optimizer, presented in the previous section. [Figure 6](#) and [Figure 7](#) depict the changes in the optimal path flow and link flow distribution under different link missing ratios. Most of the flows are distributed to the first path, since normally this is the shortest path. As the missing ratio increases from 0% to 5%, the flow will be distributed to other alternative paths (the second and third paths). The changes in path flow lead to the changes in link flow. In the [Figure 7](#), we note that when the network misses 10% of links, the flows of links 1-6 and 24 increase (red boxes), while the flows of links 48 and 53-60 decrease (green boxes).

Having generated the optimal dataset to serve as the ground truth for performance evaluation, we proceed to train the model to obtain its predictions. The training settings and hyperparameters are kept identical to those used in the previous experiment. The OD demand values and the number of OD matrices are kept constant across all experiments, with 30% of OD entries missing and a total of 4000 OD matrices generated. Scenarios 1-3 utilize the Sioux Falls network, which consists of 24 nodes and 76 links, while Scenario 4, designed to test scalability, employs the larger *Eastern Massachusetts* (EMA) network, which includes 74 nodes and 258 links. The experimental setup for each scenario is described as follows.

In *Scenario 1*, the model is trained and tested on a network with $L - j$ links, where j represents the proportion of removed links.

In *Scenario 2*, the model is first trained on the full network containing L links, and then evaluated on networks where two and three links are randomly removed ($L - 2$ and $L - 3$, respectively). These scenarios use a single-class

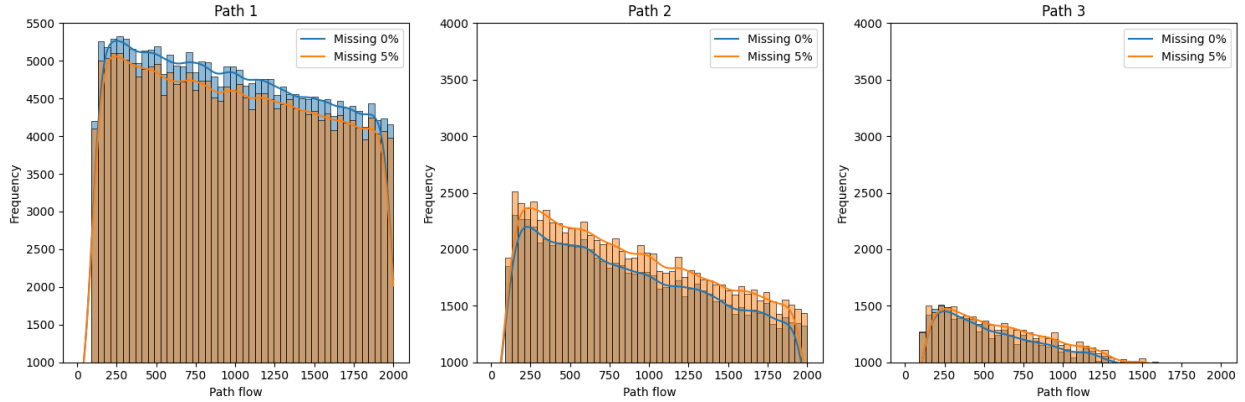


Figure 6: Histogram of optimal path flow distribution of difference link-missing ratios

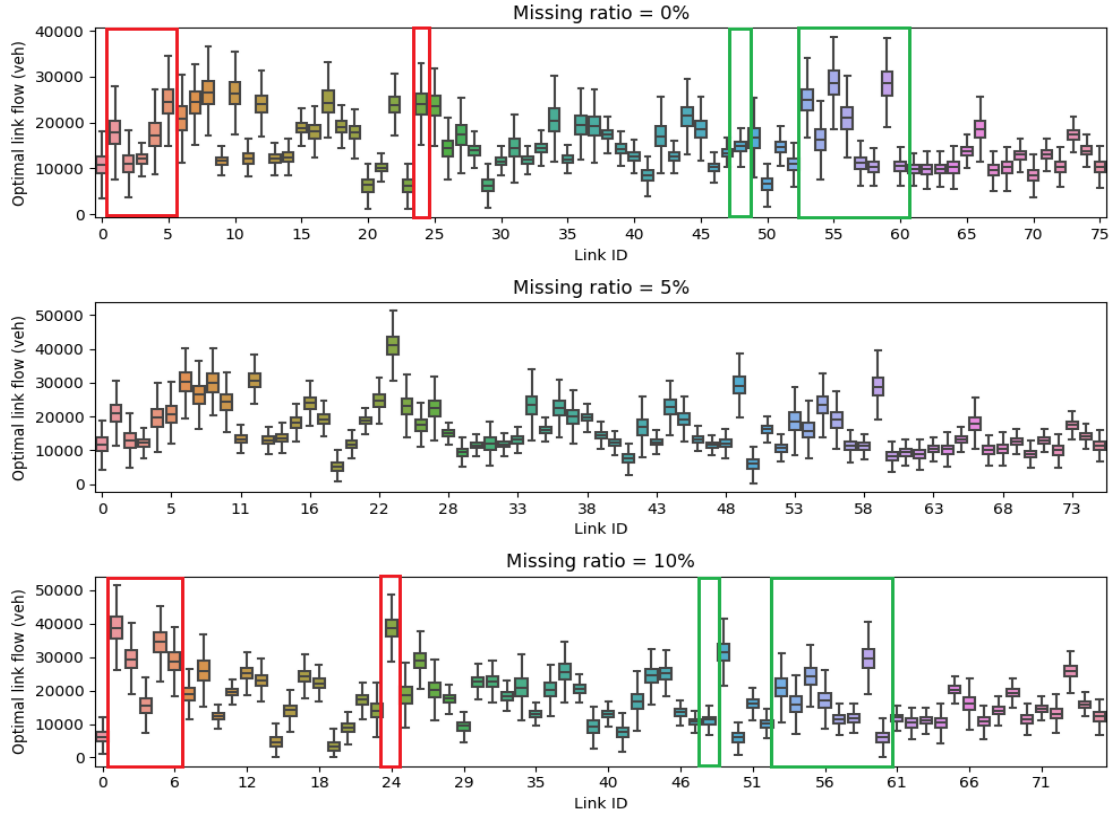


Figure 7: Boxplot of optimal link flow distribution for different link-missing ratios

network.

In *Scenario 3*, we extend the framework to a multi-class setting with $n = 2$ classes (cars and trucks). Truck demand is randomly generated as 50% of the car demand, and the free-flow travel time for trucks is set to 1.5 times that of cars. This scenario uses the full network with all L links.

In *Scenario 4*, we evaluate the scalability of the proposed framework using the larger EMA urban network. Table 7 provides detailed information about the EMA network. As this scenario focuses on assessing the model's performance with large-scale networks, we conduct a single experiment with the full network, where 50% of the demand is missing.

5.4.2. Numerical results

Scenario 1:

Table 8 summarizes the prediction performance of the model under various scenarios of missing links. It is evident that the model can predict path flow distribution even with missing links, although it performs best when no links are missing. The predicted path flows result in a network delay of 0.79% compared to the average path cost, which corresponds to a difference of 0.65 minutes relative to the optimal solution's delay. The error of predicted path flow is smaller than the error of link flow, which is aggregated from predicted path flow, with MAPE of 2.25% for path flows and 2.61% for link flows.

When the missing ratio increases to 10%, the network delay percentage also increases from 0.79% to 1.69%. Consequently, the MAPEs for the predicted path flows and the link flows increase to 3.07% and 9.06%, respectively. **Figure 8** illustrates the distribution of errors in link flow and the path flow in this scenario. The histogram is heavily skewed to the right, indicating that most errors are relatively small. For example, 95% of the predicted link flows have an absolute error of less than 479, and 95% of the predicted path flows have an absolute error under 23.

Figure 9 demonstrates the changes in the error of predicted flows at the link level as the link missing ratio increases. Note that when the link missing ratio increases to 10%, the errors of the links between nodes 8-9 and 13-24 increase significantly due to the low capacity (5050 and 5091, respectively) and the high travel demand of all the paths that pass through these links. In particular, the frequency of usage of the link between nodes 8-9 and nodes 13-24 is 179 and 175, respectively, when the link missing ratio increases to 10%. These are the highest frequency values compared to other links.

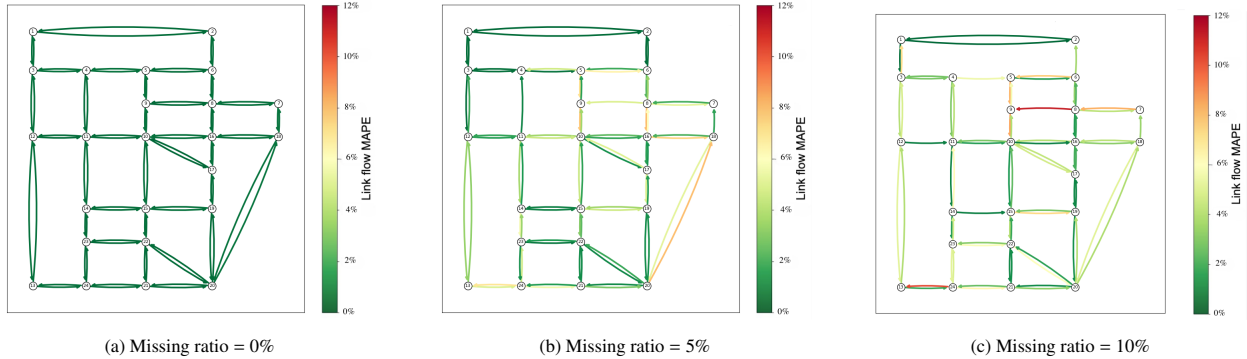


Figure 9: Heat map of link flow MAPE in different missing ratios of link

Scenario 2:

Table 9 presents the model's performance when two and three links are randomly disabled without retraining. The results demonstrate that the proposed model is capable of accurately predicting the distribution of the path flow despite minor changes in the network supply, without requiring retraining. The predicted path flow exhibits a MAPE of less than 5%, indicating high predictive accuracy with a small error. Furthermore, the average network delay associated with the predicted path flow remains low, at just 0.65%. As the number of removed links increases from two to three, the MAPE of the predicted path flow rises from 3.61% to 4.25%. The AD difference is minimal, showing the model's strong ability to predict travel times accurately.

The result demonstrates the model's capability in conducting 'what-if' analyses, particularly in scenarios where

Table 7: Eastern-Massachusetts network details

Detail	Min value	Max value
Length (miles)	1.06	32.925
Capacity (vehicle)	825	8352.013
Free flow travel time (hours)	0.016	0.88
Demand	50	500

Table 8: Model performance with Sioux Falls network under different link missing ratios

Measure	Missing ratio = 0%	Missing ratio = 5%	Missing ratio = 10%
Path flow MAE	5.02	6.93	7.37
Path flow MAPE (%)	2.25	2.98	3.07
Predicted average delay (mins)	0.71	1.96	2.15
Delay percentage (%)	0.79	1.52	1.69
AD difference (mins)	0.65	1.90	2.06

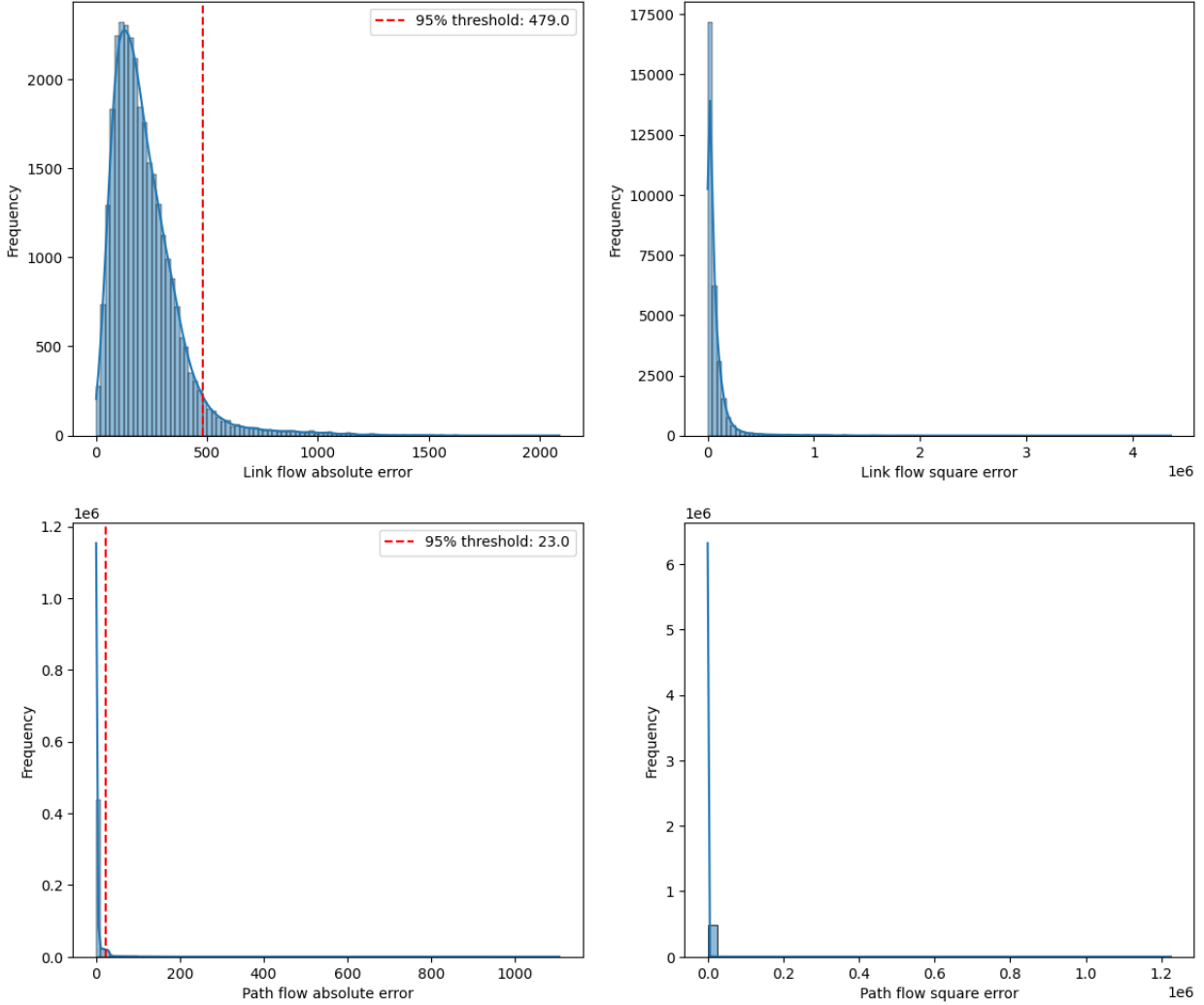


Figure 8: Histogram of link flow and path flow error

certain links are removed. For the model to function correctly, the only requirement is to ensure that at least one feasible path exists for each input OD pair.

Scenario 3:

Table 10 presents the performance of the proposed model with a multi-class traffic network (cars and trucks). The MAPE for both vehicle types is low, particularly for trucks, indicating that the model's percentage error is relatively small, suggesting a generally good fit. The model predicts the path flow for trucks more accurately than for cars, as shown by the MAPE values: 1.55% for trucks and 2.11% for cars. The delay percentage based on the predicted

Table 9: Model performance with Sioux Falls network when randomly disabling 2-3 links without retraining

Measure	2 links disable	3 links disable
MAE	8.07	8.16
MAPE (%)	3.61	4.25
Predicted average delay (mins)	0.95	1.05
Delay percentage (%)	0.63	0.65
UE Solution average delay (mins)	0.07	0.06
AD difference	0.88	0.99

path flow is also lower for trucks (0.35%) compared to cars (0.36%). In this scenario, link flow predictions are more accurate than path flow predictions (for cars, it is 1.02% and 2.11%, respectively).

Table 10: Model performance with multi-class network

Indicator	Car	Truck
MAE	4.10	1.95
MAPE (%)	2.11	1.55
Delay percentage (%)	0.36	0.35
UE Solution delay percentage (%)	0.17	0.09
AD difference (mins)	2.35	2.27

Scenario 4:

Table 11 presents the performance of the proposed model when applied to the large-scale EMA network for predicting optimal path flow. The results demonstrate that even with a network of this scale, the model achieves a low error rate, with MAPE of 3.69%. The delay percentage of the network, based on the predicted path flow, is 2.36%, only 0.21% higher than the "ground-truth" solution. This indicates that the model's predictions are closely aligned with optimal User Equilibrium (UE) conditions in terms of travel time delay. Furthermore, the model's prediction time for each OD matrix is 0.003 seconds, which is 5000 times faster than the 15-second solving time required by Gurobi.

Table 11: Model performance with EMA network (50% OD missing)

Indicator	EMA network (50% OD missing)
MAE	6.01
MAPE (%)	3.69
Delay percentage (%)	2.36
UE Solution delay percentage (%)	2.15
AD difference (mins)	24.72

For this complex problem, utilizing 4,000 samples provides an appropriate balance between avoiding overfitting and maintaining computational efficiency. A smaller sample size may increase the risk of overfitting, while a larger sample size could result in significantly higher computational costs. Given that the current framework is adaptable to both small and large-scale networks, it is not necessary to conduct experiments with a more complex framework.

6. Discussion and Conclusion

This paper presents a novel framework for UE solution prediction in the traffic assignment problem utilizing the Transformer architecture, a state-of-the-art deep learning architecture known for its efficacy in handling complex sequence modeling tasks. The motivation for this research stems from the need to overcome the computational challenges associated with classical mathematical optimization methods for UE. The proposed approach aims to predict

path flows from the user's perspective, thus providing a more granular and theoretical solution. Importantly, the model learns path flows that inherently satisfy flow conservation and OD demand, attending to physical and operational constraints without requiring explicit enforcement during training. We do not consider all possible equilibrium path flows as reference points; therefore, even if our solution deviates from other equilibrium configurations, it may still achieve better overall quality according to the selected criteria.

To validate the proposed method, we conducted experiments on both synthetic networks and real-world urban transportation networks, considering various link-missing cases and multi-class scenarios with incomplete OD demand, and on a large-scale network, demonstrating the model's effectiveness in predicting optimal path flow distributions. The results demonstrate that the model can reliably predict path flows even when both OD demand data and network link data are missing. Moreover, it maintains robust performance under network topology changes without retraining, despite being trained only on baseline missing OD demand. Thus, the framework not only reduces computational costs but also adapts to changes in network demand and structure without retraining, enabling robust 'what-if' analyses for transportation planning and management. This study demonstrates the effectiveness of an attention-based sequence learning framework in capturing complex correlations between OD pairs (Figure 1), providing a robust surrogate model capable of accelerating complex optimization tasks in areas such as resource allocation and infrastructure management.

Given the methodological focus of this study, and in view of differences in output representation and conservation treatment across existing models, direct benchmarking against state-of-the-art approaches is not pursued here. Moreover, most existing studies do not provide publicly available code or reproducible implementations, making it challenging to ensure a fair and consistent comparison within the same path-flow framework. A systematic comparative evaluation in a unified path-flow setting remains an important direction for future work. Currently, the model focuses on learning and predicting static traffic flow patterns, with the approach limited to path exploration, cost functions, and a graph-based representation. However, the framework is flexible enough to accommodate additional inputs, such as topological considerations, which could further improve equilibrium predictions. As a potential extension, the framework could be adapted to learn dynamic traffic flow patterns. Future research will explore how this model can be trained to handle time-dependent path flows.

Acknowledgments

This work was supported by the France–Berkeley Fund under the project "MADyNE" and the French ANR research project SMART-ROUTE under Grant ANR-24-CE22-7264.

References

Ameli, M., Lebacque, J.-P., Leclercq, L., 2020. Simulation-based dynamic traffic assignment: Meta-heuristic solution methods with parallel computing. *Computer-Aided Civil and Infrastructure Engineering* 35 (10), 1047–1062.

Bar-Gera, H., 2002. Origin-based algorithm for the traffic assignment problem. *Transportation Science* 36 (4), 398–417.

Beckman, M., McGuire, G., 1956. Cb winsten studies in the economics of transportation.

Bogaerts, T., Masegosa, A. D., Angarita-Zapata, J. S., Onieva, E., Hellinckx, P., 2020. A graph cnn-lstm neural network for short and long-term traffic forecasting based on trajectory data. *Transportation Research Part C: Emerging Technologies* 112, 62–77.
URL <https://www.sciencedirect.com/science/article/pii/S0968090X19309349>

Bruno, F., Fabio, S., Hector, A.-M., Paulo, N., Jose, N., Cesar, A., 2020. Long short-term memory networks for traffic flow forecasting: Exploring input variables, time frames and multi-step approaches.

Charton, F., Hayat, A., Lample, G., 2021. Learning advanced mathematical computations from examples.
URL <https://arxiv.org/abs/2006.06462>

Chen, D., Lin, Y., Li, W., Li, P., Zhou, J., Sun, X., 04 2020. Measuring and relieving the over-smoothing problem for graph neural networks from the topological view. *Proceedings of the AAAI Conference on Artificial Intelligence* 34, 3438–3445.

Dial, R. B., 2006. A path-based user-equilibrium traffic assignment algorithm that obviates path storage and enumeration. *Transportation Research Part B: Methodological* 40 (10), 917–936.
URL <https://www.sciencedirect.com/science/article/pii/S0191261506000269>

Fang, Y., Jiang, J., He, Y., 2021. Traffic speed prediction based on lstm-graph attention network (l-gat). In: 2021 4th International Conference on Advanced Electronic Materials, Computers and Software Engineering (AEMCSE). pp. 788–793.

Ford, L. R., Fulkerson, D. R., 1958. A suggested computation for maximal multi-commodity network flows. *Management Science* 5 (1), 97–101.
URL <https://doi.org/10.1287/mnsc.5.1.97>

Fukushima, M., 1984. A modified frank-wolfe algorithm for solving the traffic assignment problem. *Transportation Research Part B: Methodological* 18 (2), 169–177.

Ghaderi, A., Sanandaji, B. M., Ghaderi, F., 2017. Deep forecast: Deep learning-based spatio-temporal forecasting.

Guo, S., Lin, Y., Feng, N., Song, C., Wan, H., Jul. 2019. Attention based spatial-temporal graph convolutional networks for traffic flow forecasting. Proceedings of the AAAI Conference on Artificial Intelligence 33 (01), 922–929.

URL <https://ojs.aaai.org/index.php/AAAI/article/view/3881>

H., B.-G., B., S., E., S., 2023. Transportation networks for research core team. Transportation Networks for Research. URL <https://github.com/bstabler/TransportationNetworks>

Hamilton, W., Ying, Z., Leskovec, J., 2017. Inductive representation learning on large graphs. In: Guyon, I., Luxburg, U. V., Bengio, S., Wallach, H., Fergus, R., Vishwanathan, S., Garnett, R. (Eds.), Advances in Neural Information Processing Systems. Vol. 30. Curran Associates, Inc.

URL https://proceedings.neurips.cc/paper_files/paper/2017/file/5dd9db5e033da9c6fb5ba83c7a7ebea9-Paper.pdf

He, K., Zhang, X., Ren, S., Sun, J., June 2016. Deep residual learning for image recognition. In: Proceedings of the IEEE Conference on Computer Vision and Pattern Recognition (CVPR).

Hu, X., Xie, C., 2025. Use of graph attention networks for traffic assignment in a large number of network scenarios. Transportation Research Part C: Emerging Technologies 171, 104997.

Jafari, E., Pandey, V., Boyles, S. D., 2017. A decomposition approach to the static traffic assignment problem. Transportation Research Part B: Methodological 105, 270–296.

URL <https://www.sciencedirect.com/science/article/pii/S0191261516306403>

Jia, R., Gao, K., Liu, Y., Yu, B., Ma, X., Ma, Z., 2025. i-cltp: Integrated contrastive learning with transformer framework for traffic state prediction and network-wide analysis. Transportation Research Part C: Emerging Technologies 171, 104979.

URL <https://www.sciencedirect.com/science/article/pii/S0968090X2400500X>

Kipf, T. N., Welling, M., 2017. Semi-supervised classification with graph convolutional networks.

Li, Q., Han, Z., Wu, X.-M., 2018. Deeper insights into graph convolutional networks for semi-supervised learning. In: Proceedings of the Thirty-Second AAAI Conference on Artificial Intelligence and Thirtieth Innovative Applications of Artificial Intelligence Conference and Eighth AAAI Symposium on Educational Advances in Artificial Intelligence. AAAI'18/IAAI'18/EAAI'18. AAAI Press.

Liu, T., Meidani, H., 2024. Heterogeneous graph neural networks for end-to-end traffic assignment and traffic flow learning. Transportation Research Part C: Emerging Technologies.

Liu, T., Meidani, H., 2025. Multi-class traffic assignment using multi-view heterogeneous graph attention networks. Expert Systems with Applications 286, 128072.

URL <https://www.sciencedirect.com/science/article/pii/S0957417425016938>

Liu, X., Zhang, Y., Zhang, K., Cheng, Q., Xing, J., Liu, Z., 2025. A scalable learning approach for user equilibrium traffic assignment problem using graph convolutional networks. Electronic Research Archive 33 (5), 3246–3270.

Liu, Z., Yin, Y., Bai, F., Grimm, D. K., 2023. End-to-end learning of user equilibrium with implicit neural networks. Transportation Research Part C: Emerging Technologies 150, 104085.

Ma, X., Tao, Z., Wang, Y., Yu, H., Wang, Y., 2015. Long short-term memory neural network for traffic speed prediction using remote microwave sensor data. Transportation Research Part C: Emerging Technologies 54, 187–197.

URL <https://www.sciencedirect.com/science/article/pii/S0968090X15000935>

Mandalis, P., Chondrodima, E., Kontoulis, Y., Pelekis, N., Theodoridis, Y., 2025. A transformer-based method for vessel traffic flow forecasting. GeoInformatica 29 (1), 149–173.

Mehrabipour, M., Hajbabaie, A., 2021. A distributed gradient approach for system optimal dynamic traffic assignment.

Nishi, T., Otaki, K., Hayakawa, K., Yoshimura, T., 2018. Traffic signal control based on reinforcement learning with graph convolutional neural nets. In: 2018 21st International Conference on Intelligent Transportation Systems (ITSC). pp. 877–883.

Patriksson, M., 2015. The traffic assignment problem: models and methods. Courier Dover Publications.

Qasim, R., Bangal, W. H., Alqarni, M. A., Ali Almazroi, A., 2022. A fine-tuned bert-based transfer learning approach for text classification. Journal of Healthcare Engineering 2022 (1), 3498123.

URL <https://onlinelibrary.wiley.com/doi/abs/10.1155/2022/3498123>

Rahman, R., Hasan, S., 2023. Data-driven traffic assignment: A novel approach for learning traffic flow patterns using a graph convolutional neural network.

Skardal, P. S., Arola-Fernández, L., Taylor, D., Arenas, A., Dec 2021. Higher-order interactions can better optimize network synchronization. Phys. Rev. Res. 3, 043193.

URL <https://link.aps.org/doi/10.1103/PhysRevResearch.3.043193>

Su, Y., Fan, W., Puchinger, J., Shen, M., Jan. 2021. A Deep-Learning Approach for Network Traffic Assignment with Incomplete Data. In: Transportation Research Board 100th Annual Meeting. Washington D.C., United States.

URL <https://hal.science/hal-03131516>

Tan, H., bin Yu, C., Du, M., 2020. A multiple-path gradient projection method for solving the logit-based stochastic user equilibrium model. Journal of Transport and Land Use 13 (1), 539–558.

Vaswani, A., Shazeer, N., Parmar, N., Uszkoreit, J., Jones, L., Gomez, A. N., Kaiser, L. u., Polosukhin, I., 2017. Attention is all you need. In: Guyon, I., Luxburg, U. V., Bengio, S., Wallach, H., Fergus, R., Vishwanathan, S., Garnett, R. (Eds.), Advances in Neural Information Processing Systems. Vol. 30. Curran Associates, Inc.

URL https://proceedings.neurips.cc/paper_files/paper/2017/file/3f5ee243547dee91fdb053c1c4a845aa-Paper.pdf

W., F., Z., T., P., Y., J., X. F. . Z., 2023. Deep learning-based dynamic traffic assignment with incomplete origin–destination data.

Wang, S., Cao, J., Yu, P. S., 2022. Deep learning for spatio-temporal data mining: A survey. IEEE Transactions on Knowledge and Data Engineering 34 (8), 3681–3700.

Wardrop, J. G., 1952. Road paper. some theoretical aspects of road traffic research. Proceedings of the Institution of Civil Engineers 1 (3), 325–362.

URL <https://doi.org/10.1680/ipeds.1952.11259>

Wen, Y., Xu, P., Li, Z., Xu, W., Wang, X., 2023. Rpconvformer: A novel transformer-based deep neural networks for traffic flow prediction. Expert Systems with Applications 218, 119587.

Wu, J., He, D., Li, X., He, S., Li, Q., Ren, C., 2023. A time series decomposition and reinforcement learning ensemble method for short-term passenger flow prediction in urban rail transit.

Xue, Z., Huang, L., Ning, Q., 2025. Asttn: An adaptive spatial-temporal transformer network for traffic flow prediction. *Engineering Applications of Artificial Intelligence* 148, 110263.
URL <https://www.sciencedirect.com/science/article/pii/S0952197625002635>

Yosef Sheffi. Prentice-Hall, E. C., 1986. Urban transportation networks: Equilibrium analysis with mathematical programming methods. *Transportation Research Part A: General* 20 (1), 76–77.

Yu, B., Yin, H., Zhu, Z., Jul. 2018. Spatio-temporal graph convolutional networks: A deep learning framework for traffic forecasting. In: Proceedings of the Twenty-Seventh International Joint Conference on Artificial Intelligence. IJCAI-2018. International Joint Conferences on Artificial Intelligence Organization.
URL <http://dx.doi.org/10.24963/ijcai.2018/505>

Zhang, P., Qian, S., 2025. Low-rank approximation of path-based traffic network models. *Transportation Research Part C: Emerging Technologies* 172, 105027.

Zhou, J., Cui, G., Hu, S., Zhang, Z., Yang, C., Liu, Z., Wang, L., Li, C., Sun, M., 2020. Graph neural networks: A review of methods and applications. *AI open* 1, 57–81.